Sea ice thickness measurement and its underside morphology analysis using radar penetration in the Arctic Ocean

SUN Bo (孙 波)[1,2], WEN Jiahong (温家洪)[1], HE Maobing (何茂兵)[1], KANG Jiancheng (康建成)[1], LUO Yuzhong (罗宇忠)[1] & LI Yuansheng (李院生)[1]

1. Polar Research Institute of China, Shanghai 200129, China;
2. Laboratory of Ice Core and Cold Region Environment, Cold and Arid Regions Environmental and Engineering Institute, Chinese Academy of Sciences, Lanzhou 730000, China

Correspondence should be addressed to Sun Bo (email: sunbo@public3.sta.net.cn)

Received October 21, 2002

Abstract Based on radar penetrating measurements and analysis of sea ice in the Arctic Ocean, the potential of radar wave to measure sea ice thickness and map the morphology of the underside of sea ice is investigated. The results indicate that the radar wave can penetrate Arctic summer sea ice of over 6 m in thickness; and the propagation velocity of the radar wave in sea ice is in the range of 0.142 m • ns^{-1} to 0.154 m • ns^{-1}. The radar images display the roughness and micro-relief variation of sea ice bottom surface. These features are closely related to sea ice types, which show that radar survey may be used to identify and classify ice types. Since radar images can simultaneously display the linear profile features of both the upper surface and the underside of sea ice, we use these images to quantify their actual linear length discrepancy. A new length factor is suggested in relation to the actual linear length discrepancy in linear profiles of sea ice, which may be useful in the further study of the area difference between the upper surface and bottom surface of sea ice.

Keywords: Arctic Ocean, radar penetration, sea ice thickness, underside morphology, sea ice type.

DOI: 10.1360/02yd0033

Sea ice, as an important component of the Arctic climate system, has drawn significant scientific interest. Sea ice thickness and its morphology have dramatic impacts on ocean-atmosphere-ice interactions[1—4], which directly affect the exchange process and speed of heat and mass between the ocean and the atmosphere, dominate the physical mechanics features of sea ice, and affect the sea ice movement and deformation as well as ice freezing and melting process[5—10]. In this respect, studies on the effect of sea ice thickness and its morphology are of crucial importance.

Currently, the most useful techniques of obtaining sea ice thickness and its bottom surface morphology are upward-looking sonars either from submarines or moorings[11,12], that is, to use sub-sea sonar to measure directly upward at the sea ice canopy, ice thickness and its bottom morphology have been derived from sonar image records of ice draft and ridge keel. Drilling survey is also a reliable method to measure sea ice thickness, yet its low efficiency cannot satisfy the re-

quirements of large scale scientific sea ice investigations. Over the past 10 years, with the development of space technology, sea ice remote sensing data can be obtained via satellites and airborne surveys, these data can generate sea ice thickness and its morphology with the help of numerical models[13—15]. Yet up to now remote sensing data are very imprecise. It is the lack of adequate high quality measuring data on sea ice variations that results in the inconsistencies between the arctic and global climates simulated by different models[16—19].

Here we employed the radar penetration method to measure Arctic sea ices during July and August of 1999. The experiment area covered first-year ice and multi-year ice. In this paper, we evaluate the properties of radar penetration to measure sea ice thickness and its underside morphology, discuss the corresponding relationship between sea ice types and sea ice underside morphology reflected by radar images, and analyze the area difference between the upper surface and bottom surface of sea ice.

1 Study area and methods

China's first Arctic scientific exploration from July the 1st to September the 9th, 1999 was in the midsummer in the Arctic Ocean[20]. The temperature of the experiment area fluctuated between −5.7℃ and +6℃. Sea ice was in the strong melting season and surface snow cover has almost melted away. We chose typical ice floes to carry out radar penetrating survey experiment and drilling survey. The survey area is within the scope of N:72°23′—76°04′, W:153°36′—164°52′. Fig. 1 shows the distribution of six radar survey sites whose specific locations are listed in table 1. Sea ice types include first-year ice and multi-year ice. Radar survey experiments were conducted on level ice upper surface so as to avoid radar wave distortions caused by pressure ridge, ice stack and ice upper surface undulation, thereby the sea bottom surface morphology was prominent on the radar images.

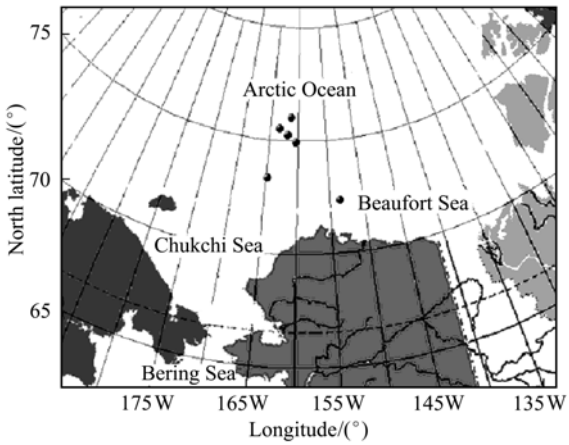

Fig. 1. Sketch map of experiment area (the dots indicate the radar survey sites).

The survey instrument is a new generation pulseEKKO 100A enhancement radar system manufactured by SSI (Sensors & Software Inc.), Canada. Having considered both the penetration and resolution performances of radar electromagnetic wave, we chose two antennas with central frequencies of 100 MHz and 200 MHz, respectively. The practical radar survey method is set up for the profiling (reflection) mode, by which the receiver antenna and the transmitter antenna are spaced at a fixed distance with the same equidistant position along a prearranged survey line to obtain radar profiles. The result of

radar survey images is qualitative statements in the form of two-way travel time versus reflected signal level. In order to validate the reliability of radar survey image to show the ice thickness and the ice bottom surface, one or two cross-borehole measurements were made on each radar survey line. Cross-borehole measurements were used for the comparison with corresponding radar survey data and providing necessary thickness data to estimate radar wave propagation velocity in sea ice.

Table 1 Comparisons of radar survey site, cross-borehole measured ice thickness, radar two-way travel time and propagation velocity

Site No.	LD001	LD002		LD003	LD004	LD005		LD006	
Date	Aug. 4	Aug. 10		Aug. 18	Aug. 20	Aug. 22		Aug. 23	
Position	73°22′ N, 164°51′ W	72°24′ N, 153°35.3′ W		74°58.4′N , 160°32.6′ W	76°3.8′ N, 161°28.8′ W	75°17.2′ N, 161°55.5′ W		75°31.2′ N, 163°28′ W	
Cross-borehole No.	BZ- 1	BZ- 2	BZ- 3	BZ- 4	BZ- 5	BZ- 6	BZ- 7	BZ-8	BZ-9
Cross-borehole measured ice thickness /m	4.00	2.85	2.30	4.85	5.40	2.65	4.42	5.67	4.16
Two way travel time/ns	56	38	31	64	70	36	61	74	55
Propagation velocity/m • ns^{-1}	0.142	0.150	0.148	0.152	0.154	0.147	0.145	0.153	0.151

2 Analysis of radar penetration to sea ice and its propagation velocity

By using radar to measure sea ice thickness and display its bottom surface morphology, the key lies in the penetration performance of electromagnetic wave to sea ice, meanwhile it also depends on the performance of radar image to display the ice/water interface. We conducted an on-site experiment to analyze and test the penetration performance of radar wave to sea ice. We estimated the real propagation velocity of radar wave in sea ice by comparing radar profile results with cross-borehole data.

First, we have repeated tests on experimental sea ice surface to determine radar antennas with appropriate frequency and best survey parameters. Then, we conducted radar field surveys and drilling surveys at six sites. Altogether about 4 km long radar survey profile data and 9 cross-borehole survey data have been collected. Fig. 2 is a typical radar image taken at survey site LD003.

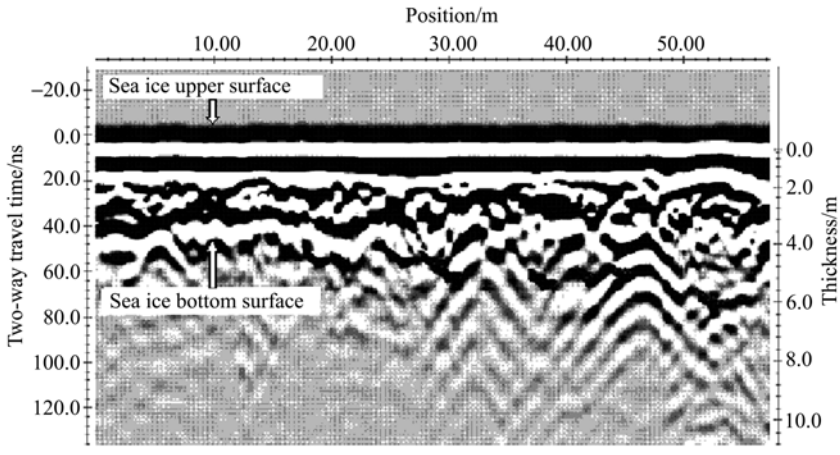

Fig. 2. A section of radar penetration survey profile from Arctic sea ice.

This image can visually be divided into the upper, middle and bottom areas. The bold black line separates the clean and identical upper area from the fluctuating and ripple middle area. In the bottom area, the ripples decrease markedly until none. We use radar survey theories and sea ice property to explain the above image characteristics. The upper area image reflects various electromagnetic background disturbances. The clean and identical image indicates that radar survey process has received no electromagnetic noise signal disturbance, which is the prerequisite of successful radar surveys. The middle area image reflects the rich echo signals generated when radar wave penetrates into sea ice. It displays the distinct and fluctuating layers within sea ice. This is consistent with the possible influence of the complex sea ice components, structures and temperatures on radar wave. The bottom area image reflects the strong attenuation and weakening of radar wave energy. This is consistent with sea water's strong absorption of electromagnetic waves. There is a clear-cut line between middle and bottom areas. It can be only attributable to two possibilities. The first possibility is that there exists a continuous and very strong reflection layer in sea ice medium. It prevents the penetration of radar wave. The second possibility is mainly due to the distinct electromagnetic difference between sea ice and sea water. In order to reveal the real reason for this line, we examined and analyzed the ice layer features of the extracted cores. There was no obvious borderline between layers except normal year-layer development. Moreover, analysis on comparison between on-site borehole measured data and radar profile data (as shown in table 1) indicates that the two way travel time is well related to the borehole measured sea ice thickness. Thicker sea ice corresponds longer two way travel time, and on the contrary, thinner sea ice corresponds shorter transmission time. Through regression analysis of these two, the results show that there is a good linear correlation between two way travel time and sea ice thickness (as in fig. 3.).

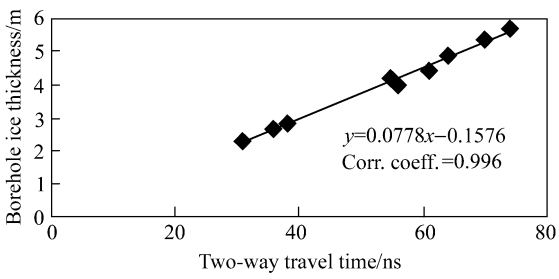

Fig. 3. Relationship between two way travel time and sea ice thickness.

We assume that the two way travel time in table 1 is what radar wave needs to penetrate sea ice, then, we can figure out the propagation velocity of radar wave via the cross-borehole measured ice thickness and the two way travel time of radar wave. If the propagation velocity was in accord with the former study results, then we could exclude the 1st possibility for the above borderline in radar image, and then the 2nd possibility became the only choice. So we use the formula $v = 2h/t_s$, where v is propagation velocity, h is cross-borehole measured ice thickness, t_s is the two way travel time of radar wave penetrating sea ice, to calculate the total 9 group data of the cross-borehole measured ice thickness and corresponding propagation time of radar wave. The result (as in table 1) shows that the propagation velocity of radar wave in midsummer Arctic sea ice is within the range of 0.142—0.154 m • ns^{-1}. Kovas and Morey[21—23] analyzed and calculated the

propagation velocity of radar wave in midsummer Arctic sea ice and the resulting range of 0.138—0.160 m • ns^{-1}. We can find that the propagation velocity estimated in this paper is in accordance with the former studies, and then we can confirm that the clear borderline in the radar image is the ice/water interface.

Therefore, as electromagnetic property of sea ice differs sharply from that of sea water, there is obvious difference between radar wave propagation in sea ice and that in sea water, and a sharp radar wave reflection layer between sea ice and sea water has been formed. For the sea ice part, rich reflecting echo phenomenon is reflected in radar image, while for sea water part, it presents the phenomenon of strong attenuation and absorption. It is because of the remarkable difference between the radar image of sea ice and that of sea water (as in fig. 2) that the position and micro-morphology of sea ice bottom surface can be completely displayed, which adequately shows that radar wave can not only penetrate sea ice, but also visually show the position and morphology of ice/water interface in radar image.

Cross-borehole measured ice thickness showed that the thickness of sea ice in the test area is between 2.30 m and 5.67 m, and the value of thickest sea ice was obtained at LD006. Although the thickness of sea ice in test area was limited, we could not obtain the maximum penetration performance of radar electromagnetic wave in sea ice. Considering that radar images display good intensity feature of radar wave reflecting echo signal, combined with theory analysis of radar equation, we are sure that if the proper frequency antenna and best survey parameters are chosen, the penetrating thickness of sea ice by radar wave is at least over 6 m. Given the average velocity 0.150 m • ns^{-1} of radar wave propagation in sea ice, based on the velocity data in table 1, ice thickness can be directly calculated from radar profile. Table 2 shows the results of ice thickness comparison between cross-borehole measurement data and radar profiles. From table 2, we can see the error of ice thickness derived from radar profiles is not more than 5%. So radar penetration survey is effective for sea ice thickness measurements.

Table 2 Comparison of ice thickness between cross-borehole measurement and radar profile

Cross-borehole No.	Cross-borehole ice thickness /m	Radar profile ice thickness /m	Error (%)
BZ-1	4.00	4.2	5.0
BZ-2	2.85	2.86	0.3
BZ-2	2.30	2.33	1.3
BZ-4	4.85	4.80	1.0
BZ-5	5.40	5.25	2.8
BZ-6	2.65	2.70	1.9
BZ-7	4.42	4.57	3.4
BZ-8	5.67	5.55	1.6
BZ-9	4.16	4.12	1.0

3 Sea ice bottom surface micro-morphology and sea ice type recognition

The morphology of sea ice bottom surface (ice/water interface) include distribution of ice ridge (keel) and rough and fluctuating micro-relief. They are an integrator of ocean-atmosphere-

ice interaction. The morphology is a sensitive indicator of sea ice thermodynamic growth, ice motion, and mechanical redistribution. Meanwhile, it mainly influences the thermohaline circulation of the ocean, and it is also the dominant factor which decides seawater drag coefficient[24—26]. Previous studies have drawn much attention to the roughness of sea ice bottom surface, and made significant achievement[27—29]. But those studies employed sonar methods to conduct upward or sidescan to get analysis data. Due to lower resolution of sonar measurement, they could only study the pressure ridge keel of sea ice bottom surface, and there have been few reports on the study of the rough and fluctuating micro-relief features of sea ice bottom surface up to now. In this work, we used the method of radar penetration survey, whose resolution is obviously better than that of sonar method. Radar wave can not only distinguish the distribution of pressure ridge keel of sea ice bottom surface, but also differentiate the developing status of small-scale micro-relief. The difference from the past studies is that this work focused on the analysis and study of micro-relief features of sea ice bottom surface.

Radar profiles showed that the micro-morphology of sea ice bottom surface could be clearly presented on the ice/water interface in radar images, and different types of sea ice display clearly different morphologies, as shown by the example in fig. 4.

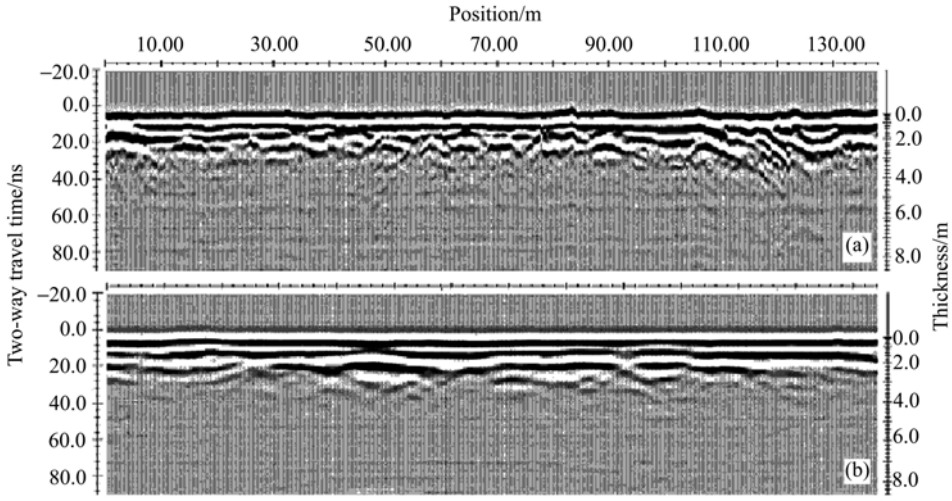

Fig. 4. Comparision of morphology of Arctic summer sea ice bottom surface. (a) Multi-year ice; (b) first-year ice.

Fig. 4 includes the radar profile results of multi-year floe (a) and first-year floe (b). Fig. 4(a) shows the toothed and wrinkled feature of sea ice bottom surface, while fig. 4(b) shows that the bottom surface is smooth and flat, and there is no knaggy change. From the analysis of ice core crystal structure profile, we find that the ice core sample drilled from ice floe (a) presents the characteristics of alternant distribution between granular and column ice layers from top to bottom, which can be concluded as a typical multi-year ice floe . And the ice core sample drilled from ice floe (b) presents a layer of granular ice crystal and a layer of column ice crystal from top to bot-

tom, which belongs to typical first-year ice floe. The main reasons why micro-morphology of sea ice bottom surface unveiled by radar images correspond well with sea ice types are as follows: The first-year sea ice experiences short time affection by sea current and wind with insufficient freezing and desalination process, hence smooth bottom surface; in the process of multi-year ice development, the action of long-time sea current and wind makes the sea ice bottom surface coarse. Meanwhile, in the process of freezing and desalination of sea ice and the change of ice components and structures, together with the phenomenon of melting water infiltration and gravity transfer during sea ice evolvement process, the morphology of knaggy sea ice bottom surface becomes more complex.

Basing on the good corresponding relation between micro-morphology of sea ice bottom surface and sea ice types (ice age), and the fact that radar images can clearly display micro-morphology of sea ice bottom surface, we conclude that radar penetrating survey may be an effective method to distinguish first-year and multi-year sea ice types.

4 Difference analysis of effective area of upper surface and bottom surface of multi-year ice

It is the common knowledge that the upper surface of sea ice is the interface between ice and air, while the bottom surface is the interface between ice and sea water, and on these two interfaces there are consistent exchange processes between material and energy. Based on the morphology of knaggy sea ice bottom surface presented by radar images, it is thought that this kind of ice bottom surface morphology might probably produce increscent effective contact area between sea ice and sea water.

Since radar image can simultaneously display upper surface and bottom surface of sea ice along radar survey line, we can analyze the cross-section length difference between upper surface and bottom surface of sea ice. What we need to explain is that, since the ice floes we chose are all level ice with smooth upper surface, and the morphology of multi-year bottom surface is more undulating than that of first-year bottom surface, this paper focuses on the multi-year sea ice with smooth upper surface. As is shown in figs. 2 and 3 for multi-year ice floes with smooth surface, radar images display the upper interface of sea ice as a smooth straight line, while the bottom interface of sea ice is displayed as a knaggy curved line. To measure the cross-section real length of upper and bottom interfaces along radar survey line, especially to resolve the problem of measuring anomalous curve line of sea ice bottom surface, we print the radar image to transparency film, making use of the amplifying imaging principle of optics projection. It is easy to get the large-size radar images without any deformation in the projection curtain, then we can accurately measure the cross-section length of upper surface and bottom surface interfaces along the radar survey line with a scale. The results are shown in table 2. To quantitatively describe the different cross-section lengths of upper surface and bottom surface interfaces, here we introduce the cross-section length factor r, which is defined as

$$r = \frac{L_b}{L_t}. \tag{1}$$

In this formula, L_b represents the cross-section real length of bottom surface interface along radar survey line, and L_t represents the cross-section real length of upper surface interface along radar survey line. The results of statistic data are present in table 3.

Table 3 Statistics of the cross-section real lengths of upper surface and bottom surface interfaces of multi-year sea ice along radar survey line

Site No.	LD001	LD002	LD003	LD004	LD005	LD006
L_b/m	381.5	77.0	992.0	2616.5	1624.0	1878.5
L_t/m	282.0	58.0	792	1984.5	1205.0	1412.5
r	1.35	1.33	1.25	1.32	1.35	1.33

Table 3 shows that length factor r is in the range of 1.25—1.35, the average value of r is 1.32, variance is 0.0013, which adequately show that there was obvious difference between upper surface and bottom surface interfaces of sea ice. If using radar grid survey to measure ice floe, then we could analyze and estimate the area difference between upper surface and bottom surface interfaces. This shows that, there are certain defects in the present modeling studies of sea ice, in which the area difference of the upper surface and the bottom surface of multi-year sea ice[30] is neglected. We should add a new factor to express the effect of area increment that may improve the analysis precision of sea ice modeling.

5 Discussion

As mentioned above, radar wave can penetrate over 6 m thick midsummer Arctic sea ice and clearly displays the position of water/ice interface. As for thickness error, radar survey is similar to the earthquake reflection survey and sonar survey. Sea ice thickness can be calculated via sea ice radar propagation velocity, that is, sea ice thickness $h = v \times t_s /2$, where v is radar wave propagation in sea ice, t_s is the two-way travel time of radar wave. Therefore, radar survey precision depends on the accuracy of radar wave two-way travel time and propagation velocity. The radar data sampling time is set as 0.8 ns, so radar survey time error is negligible. As for propagation, it should be based on specific situations. As stated above, the error of ice thickness derived from radar profiles is not more than 5%. Therefore, radar penetration survey to sea ice thickness can be resolved with high accuracy. Because radar survey error directly depends on the accuracy of radar wave propagation velocity, the most ideal way to improve radar survey accuracy is to obtain cross-borehole measured ice thickness data on each radar survey line, which is used to calculate the real propagation velocity of radar wave in sea ice. Since sea ice is an integrator of atmospheric and oceanic effects, these effects, together with sea ice motion and deformation, have caused inconsistence in sea ice composition and internal structure as well as variance in sea ice temperature. The results of sea ice electromagnetic parameters measured *in situ* are discrete, which makes it impossible to accurately deduce the radar wave penetration depth and propagation velocity by

means of electromagnetic theory and radar equation[31]. The significance of using radar wave to measure sea ice thickness lies in that this survey method is not only of high resolution and fast speed, but also easy to measure ice thickness distribution along radar survey line, which cannot be realized and substituted by drilling survey or any other methods. Although our radar survey was conducted on surface-based measurements, yet it has reference value to the future development of space and airborne radar technology so as to investigate the distribution of sea ice thickness on greater scale.

To reliably identify sea ice types is very important in the analysis of ocean-ice-atmosphere interactions and sea ice modeling. It is also indispensable to validate remote sensing data. Although it was pointed out that sea ice bottom surface is the result of sea ice growth, and hence a good indicator to recognize sea ice types, yet there lack efficient methods to measure the characteristics of sea ice bottom surface, previous methods to recognize sea ice types were made according to sea ice upper surface features such as roughness, melting pool, ice ridge development and ice salinity. The micro-morphology of sea ice bottom surface has seldom been studied in the past. This paper has already indicatecd that sea ice bottom surface micro-morphology displayed by radar image have good corresponding relationships with sea ice types. This shows that radar penetration survey is a useful method to study the micro-morphology of sea ice bottom surface. In this respect, we suggest that sea ice bottom surface micro-morphology obtained by radar penetration survey may be taken as valuable evidence to more accurately identify sea ice types.

Since the sea ice floes we chose to conduct radar survey are undeformed and flat, the possible impacts of ice ridge on radar survey is avoided. Due to the high resolution, radar survey clearly displays the zigzag feature of multi-year ice floes bottom surface. We could directly measure the real lengths of the same profile's upper and bottom interface lines, and realize the quantitative analysis of sea ice bottom surface morphology. The fluctuating feature of multi-year sea ice bottom surface would definitely bring two results: first, the real area of ice/water interface is larger than that of ice/air interface; second, it would affect the momentum processing of sea ice and ocean. Therefore, special attention should be paid to these issues during the studies of ice/water interaction and related modeling analysis in the Arctic Ocean.

Acknowledgements This work was supported by the National Natural Science Foundation of China (Grant No. 40071022), the Ministry of Science and Technology of China (Grant No.2001DIA50040), Chinese Arctic Expedition Foundation and the Laboratory Foundation of Ice Core and Cold Region Environment, Cold and Arid Regions Environmental and Engineering Institute, the Chinese Academy of Sciences (Grant No. BX2001-04).

References

1. Wadhams, P., Sea ice thickness changes and their relation to climate, in The Polar Oceans and Their Role in Shaping the Global Environment (eds. Johannessen, O. M., Muench, R. D., Overland, J. E. et al.), Geophysical Monograph, 85, Washington, DC: American Geophysical Union, 1994, 358—361.
2. Barry, R. G., Serreze, M. C., Maslanik, J. A. et al., The Arctic sea ice-climate system: Observations and modeling, Reviews of Geophysics, 1993, 31(4): 397—422.
3. Dickson, B., All change in the Arctic, Nature, 1999, 397: 389—391.
4. Padhams, P., Norman, D. R., Further evidence of ice thinning in the Arctic Ocean, Geophysical Research Letters, 2000,

27(24): 3937—3942.
5. Holland, M. M., Curry, J. A., Schramm, J. L., Modeling the thermodynamics of a sea ice thickness distribution (2): Sea ice/ocean interactions, Journal of Geophysical Research, 1997, 102: 23093—23107.
6. Huang, J. Y., Zhang, T., The effects of polar ice on South Oscillation, Acta Meteorological Sinica (in Chinese), 1997, 55(2): 200—209.
7. Xie, S. M., Bao, C. L., Hao, C. J., Interaction between sea ice of Arctic and Antarctic, Chinese Science Bulletin, 1995, 40(20): 1713—1718.
8. Goose, H., Fichefet, T., Importance of ice-ocean interactions for the global ocean circulation: A model study, Journal of Geophysical Research, 1999, 104(c10): 23337—23355.
9. Wu, H. D., Bai, S., Zhang, Z. H., Numerical analysis of sea ice dynamic process, Marine Sciences, 1998, 20(2): 1—13.
10. Steele, M., Flato, G., Sea ice growth, melt, and modeling: A review, in The Freshwater Budget of the Arctic Ocean (eds. Lewis, E. L., Jones, E. P., Lemke, P. et al.), Dordrecht, Netherlands: Kluwer Academic Publishers, 2000, 549—587.
11. Hudson, R., Annual measurement of sea-ice thickness using an upward-looking sonar, Nature, 1990, 344: 135—137.
12. Kerr, R. A., Will the Arctic Ocean lose all its ice? Science, 1999, 286: 1828.
13. Guo, F. L., Zhao, R. Y., Wang, W. B., Application of passive microwave remote sensing to sea ice thickness measurement, Journal of Remote Sensing (in Chinese), 2000, 4(2): 112—117.
14. Jin, Y. Q., Chen, Y., Zhang, W. et al., Observations of Radarsat SAR and DMSP SSM/I over sea ice of China's Bohai Sea, Chinese Journal of Geophysics (in Chinese), 2001, 44(2): 163—170.
15. Johannesen, O. M., Shalina, E. V., Miles, M. W., Satellite evidence for an Arctic sea ice cover in transformation, Science, 1999, 286: 1937—1939.
16. Lemke, P., Hibler, W. D., Flato, G. et al., On the improvement of sea-ice models for climate simulations: The sea ice model intercomparison project, Annual of Glaciology, 1997, 25: 183—187.
17. Hilmer, M., Lemke, P., On the decrease of Arctic sea ice volume, Geophysical Research Letters, 2000, 27(22): 3751—3763.
18. Zhang ,Y. X., Hunke, E. C., Recent Arctic change simulated with a coupled ice-ocean model, Journal of Geophysical Research, 2001, 106: 4369—4390.
19. Maslowski, W., Newton, B., Schlosser, P. et al., Modeling recent climate variability in the Arctic Ocean, Journal of Geophysical Research, 2000, 27: 3743—3746.
20. Chinese First Arctic Expedition Team (ed.), Report on Chinese First Arctic Expedition (in Chinese), Beijing: China Ocean Press, 2000, 70—86.
21. Kovas, A., Morey, R. M., Electromagnetic measurements of a second-year sea ice floe, in Port and Ocean Engineering Under Arctic Conditions (POAC 88) (ed. Sackinger, W. M.), 1988, 1: 121—136.
22. Morey, R. M., Kovacs, A., Cox, G. F. N., Electromagnetic properties of sea ice, Cold Regions Science and Technology, 1984, 9: 53—75.
23. Kovacs, A., Morey, R. M., Electromagnetic measurements of multi-year sea ice using impule radar, Cold Regions Science and Technology, 1986, 12: 67—93.
24. Bjørgo, E., Johanessen, O. M., Miles, M. W., Analysis of merged SMMR-SSM/I time series of Arctic and Antarctic sea ice parameters 1978—1995, Geophysical Research Letters, 1997, 24(4): 413—416.
25. Bourke, R., Mclaren, A., Contour mapping of Arctic basin ice draft and roughness parameters, Journal of Geophysical Research, 1992, 97(c11): 17715—17728.
26. Timco, G. W., Burden, R. P., An analysis of the shapes of sea ice ridges, Cold Regions Science and Technology, 1997, 25: 65—77.
27. Wadhams, P., The underside of Arctic sea ice image by sidescan sonar, Nature, 1988, 333: 161—164.
28. Kwok, R. K., Rignot, E., Holt, B. et al., Identification of sea ice types in spaceborne synthetic aperture radar data, Journal of Geophysical Research, 1992, 97(C2): 2391—2402.
29. Remund, Q. P., Long, D. G., Drinkwater, M. R., An interactive approach to multisensor sea-ice classification, IEEE Transactions on Geoscience and Remote Sensing, 2000, 38(4): 1843—1856.
30. Bitz, C. M., Holland, M. M., Weaver, A. J. et al., Simulating the ice-thickness distribution in a coupled climate model, Journal of Geophysical Research, 2001, 106: 2441—2464.
31. Kova , A., Morey, R. M., Cox, G. F. N., Modeling the electromagnetic property trends in sea ice, Part I, Cold Regions Science and Technology, 1987, 14: 207—235.